2018

Experimental Evaluation for an Extremum Seeking Control Strategy based on Input-output Correlation with a Mini-split Air Conditioning System

Zhongfan Zhao
University of Texas at Dallas, United States of America, zxz124130@utdallas.edu

Tim Salsbury
timothy.i.salsbury@jci.com

John M. House
Johnson Controls, Inc., john.m.house@jci.com

Yaoyu Li
University of Texas at Dallas, United States of America, yaoyu.li@utdallas.edu

Experimental Evaluation for an Extremum Seeking Control Strategy based on Input-output Correlation with a Mini-split Air Conditioning System

Zhongfan Zhao[1]*, Timothy I. Salsbury[2], John M. House[3], Yaoyu Li[4]

[1]The University of Texas at Dallas, Department of Electrical Engineering,
Richardson, Texas 75080, USA
E-mail: zhongfan.zhao@utdallas.edu

[2]Johnson Controls, Inc., Building Efficiency Research Group,
Milwaukee, WI 53201, USA
E-mail: Timothy.I.Salsbury@jci.com

[3]Johnson Controls, Inc., Building Efficiency Research Group,
Milwaukee, WI 53201, USA
E-mail: John.M.House@jci.com

[4]The University of Texas at Dallas, Department of Mechanical Engineering,
Richardson, Texas 75080, USA
E-mail: yaoyu.li@utdallas.edu

*Corresponding Author

ABSTRACT

Extremum Seeking Control (ESC) has emerged as a model-free real-time optimization framework, typically based on dither-demodulation driven gradient estimation. However, conventional ESC (CON-ESC) suffers from slow convergence (Moase et al. 2015). Salsbury et al. (2017) recently proposed an input-output correlation based ESC (IOC-ESC) strategy based on a statistical analysis. This study presents findings from an experimental evaluation for the IOC-ESC strategy with a ductless mini-split air conditioning system, compared with conventional ESC. This AC system has variable-capacity compressors and variable-speed evaporator and condenser fans. Both single-input and multi-input ESCs are tested in our study. The evaporator and condenser fan speeds are the manipulated variables and the total power consumption is used as feedback for all cases. This paper compares the performance of CON-ESC and IOC-ESC based on the test results.

1. INTRODUCTION

Extremum seeking control (ESC) is a form of adaptive control where the steady-state input-output characteristic is optimized, without requiring any explicit knowledge about this input-output characteristic other than that it exists and that it has an extremum (Tan et al. 2010). Conventional ESC (CON-ESC) uses periodic perturbation for which a time-scale separation is required between the fast transients of the system dynamics and the slow quasi steady-state characteristic during the extremum-seeking process. An undesirable consequence for such time-scale separation is slow convergence. Many efforts have been made to improve the convergence of ESC. Moase et al. (2010) introduced a Newton-based ESC, where the second-order derivative of the input-output map was estimated in a Newton-like continuous-time algorithm for the single-input case. Ghaffari et al. (2012) presented a Newton-based ESC algorithm for the multivariable case. A fast extremum-seeking approach for a class of Wiener-Hammerstein processes was proposed by Moase et al. (2012). Guay et al. (2017) introduced a proportional-integral ESC (PI-ESC) framework which minimizes the impact of time scale separation on the transient to the steady-state optimum.

Gelbert et al. (2012) proposed a method of using extended Kalman-filters (EKF) for gradient estimation which is accomplished using combination of high- and low-pass filters in conventional algorithm. Hunnekens et al. (2014) presented a novel type of ESC which uses the linear regression of input-output data to estimate the gradient of the performance map.

Salsbury et al. (2017) developed an ESC algorithm based on input-output correlation (IOC-ESC), which is an extension to the linear-regression idea of Hunnekens et al. (2014). In this approach, the gradient feedback variable is replaced with a normalized correlation coefficient so that it is scale-independent, and a recursive estimation procedure based on sample statistics is used, making the algorithm easy to implement. This algorithm was tested with both a numerical model in Matlab/Simulink and a Dymola model of an air conditioning system. IOC-ESC is shown to converge faster than CON-ESC.

The purpose of this paper is to evaluate the performance of IOC-ESC with experiments on a mini-split air-conditioning system, benchmarked against the CON-ESC. The remainder of the paper is organized as follows. In Section 2, we review the IOC-ESC algorithm. The experimental setup is described in Section 3. The experimental study is presented in Section 4, and the performance of IOC-ESC is compared with that of the CON-ESC. Section 5 concludes the paper with future work discussed.

2. REVIEWS OF IOC-ESC METHOD

The primary objective of this paper is to perform an experimental evaluation of the IOC-ESC method. The design of IOC-ESC algorithm is reviewed in this section. The IOC-ESC strategy proposed by Salsbury et al. (2017) is depicted in Fig. 1. For the single-input case, the static map of the plant with input u and output y_p is assumed to be convex with an extremum point at (u^*, y_p^*). The plant output is subject to a disturbance signal d and the measurable signal is y . With the assumption of (quasi) steady-state operation, we can ignore the plant dynamics and focus only on the static non-linearity which is defined as $y = f(u)$. Consider $\mathbf{u}$ to be a time series batch of u values and $\mathbf{y}$ to be a batch of y values, then we can define the correlation coefficient between $\mathbf{u}$ and $\mathbf{y}$ as:

$$\rho = \frac{Cov(\mathbf{u},\mathbf{y})}{\sigma_u \sigma_y} \tag{1}$$

We can also define the slope of a linear regression between y and u as:

$$\hat{\beta} = \frac{Cov(\mathbf{u},\mathbf{y})}{\sigma_u^2} \tag{2}$$

thus:

$$\rho = \hat{\beta}\frac{\sigma_u}{\sigma_y} \tag{3}$$

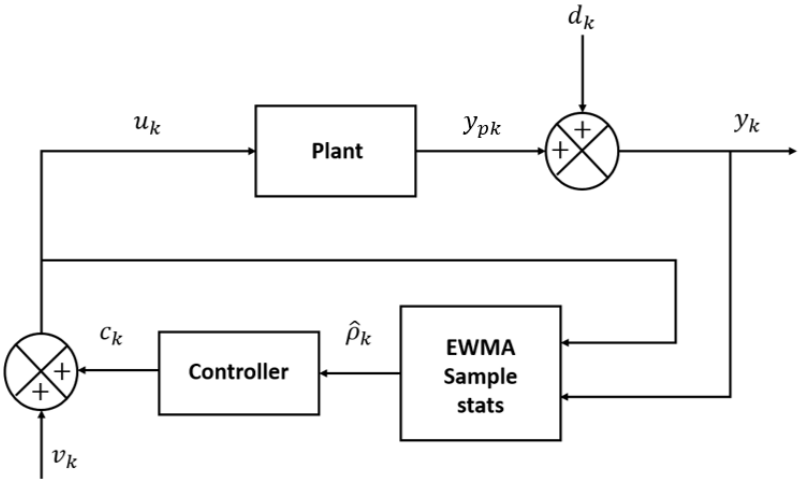

Figure 1: Block diagram of IOC-ESC method

The slope of the linear regression line will approximate the gradient of $f(u)$ and will thus have a minimum absolute value of zero when there is a local extremum in $f(u)$. The correlation coefficient $\rho \in [-1, 1]$ is estimated based on sample statistics which are calculated using exponentially-weighted moving averages (EWMAs) (Finch 2009). $\overline{u}_k$ is an estimate of the mean of u at the k-th step over window of length W with exponential forgetting factor, $\overline{y}_k$ is an estimate of the mean of y over the exponentially forgetting window of length W, $s_{u,k}^2$ and $s_{y,k}^2$ are the variance estimates of u and y, cov_k is the covariance, and $\hat{\rho}_k$ is the estimated correlation coefficient.

$$\overline{u}_k = \overline{u}_{k-1} + \frac{(\overline{u}_k - \overline{u}_{k-1})}{\min(k, W)} \tag{4}$$

$$\overline{y}_k = \overline{y}_{k-1} + \frac{(\overline{y}_k - \overline{y}_{k-1})}{\min(k, W)} \tag{5}$$

$$\text{cov}_k = \text{cov}_{k-1} + \frac{(s_{uy,k} - \text{cov}_{k-1})}{\min(k, W) - 1} \tag{6}$$

$$s_{u,k}^2 = s_{u,k-1}^2 + \frac{((u_k - \overline{u}_k)(u_k - \overline{u}_{k-1}) - s_{u,k-1}^2)}{\min(k, W) - 1} \tag{7}$$

$$s_{y,k}^2 = s_{y,k-1}^2 + \frac{((y_k - \overline{y}_k)(y_k - \overline{y}_{k-1}) - s_{y,k-1}^2)}{\min(k, W) - 1} \tag{8}$$

$$s_{uy,k} = \frac{1}{2}((y_k - \overline{y}_{k-1})(u_k - \overline{u}_k) + (y_k - \overline{y}_k)(u_k - \overline{u}_{k-1})) \tag{9}$$

$$\hat{\rho}_k = \frac{\text{cov}_k}{\sqrt{s_{u,k}^2 s_{y,k}^2}} \tag{10}$$

The estimated correlation coefficient is used as the feedback signal in the ESC control loop, which is driven to zero by adjustment of the manipulated input. An integral controller is used in the IOC-ESC loop and the error signal for the controller is the negative value of the estimated correlation coefficient and the controller expression is:

$$c_k = c_{k-1} - \tanh^{-1}(\rho)\frac{\Delta t}{\kappa \hat{\tau}_p} \tag{11}$$

where $\hat{\tau}_p$ is an estimate of the effective plant time constant, κ is a tuning factor and Δt is the sampling interval. In order to produce consistent performance across different plants, c_k should be mapped onto the range of the manipulated plant input:

$$c_k' = u_{\min} + c_k(u_{\max} - u_{\min}) \tag{12}$$

where c_k' is the scaled version of c_k. $u_{\max}$ and $u_{\min}$ are the maximum and minimum level of u, respectively.

There are two types of dither signals (v_k) considered by Salsbury et al. (2017) for the IOC-ESC: sinusoidal and aperiodic stochastic signals. The sinusoidal perturbation is defined as:

$$v(t) = a\sin\left(\frac{2\pi}{\gamma \tau_p} t\right) \tag{13}$$

a is the amplitude. $\gamma > 1$ is a design parameter. The aperiodic stochastic follows a colored noise as

$$v_k = \phi_n v_{k-1} + w_k \qquad (w_k \sim \mathbf{N}(0, \sigma_w{}^2)) \tag{14}$$

where $\phi_n = \exp\left(\frac{\Delta t}{\gamma \tau_p}\right)$ and $\sigma_w{}^2 = \left[1 - \exp\left(\frac{-2\Delta t}{\gamma \tau_p}\right)\right]\frac{a^2}{2}$.

Three major design parameters can all be determined from a specification of the estimated plant time constant τ_p:

1. Window length W is related to the sample size of the EWMA statistics. Based on empirical tests across a range of different systems, a practical guideline for selecting W is $15 \le W \le \frac{\hat{\tau}_p}{3\Delta t}$.

2. Parameter κ determines the aggressiveness of the feedback controller. A suggested value is 30.
3. Parameter γ defines the frequency characteristic of the dither signal which is generally lower than the cut-off frequency of the plant dynamics.

In the experimental study in Section 4, the tuning-factor parameter κ is denoted as TF, and τ_p is denoted with TC. Amplitude a is normalized to a_{norm} with respect to the range of the corresponding manipulated input.

3. DESCRIPTION FOR EXPERIMENTAL FACILITY

The experimental study is carried out with a 9000 BTU variable-speed mini-split ductless air conditioning (AC) system (Mitsubishi MSZ-GE09NA and MUYGE09NA) described in Xiao et al. (2014) and shown in Figure 2. The zone temperature is regulated to its setpoint using the manufacturer's controller to manipulate the compressor speed. The data acquisition and control algorithms are implemented on a National Instruments CompactRIO platform. The CompactRIO reads the power consumption measurement from the power meter, as well as the measurements of the evaporator fan and condenser fan speed. This system was previously used for evaluation of single-input and multi-variable ESC strategies by Xiao et al. (2014). This setup allows the development of supervisory controllers such as ESC that can optimize the evaporator and condenser fan speeds individually or simultaneously in real time.

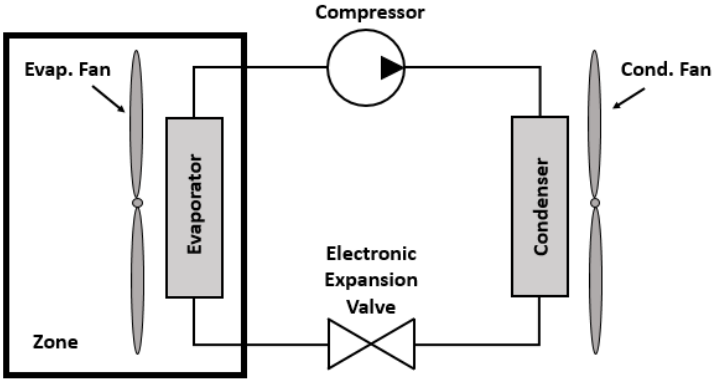

Figure 2: A simplified diagram of a mini-split AC system. There are four main components: 1) Compressor, 2) Electronic Expansion Valve (EEV), 3) Evaporator Fan, 4) Condenser Fan

An Acuvim-CL-D-5A-P1 power meter is used for power measurement, which features a serial communication interface with the controls platform. The data can be effectively transmitted over long distances with good noise immunization. To control the condenser fan motor and evaporator fan motor, the circuits are customized with a speed sensor OMEGA HHT13 and digital output module NI9474. Figure 3 shows the connections and communications among different components.

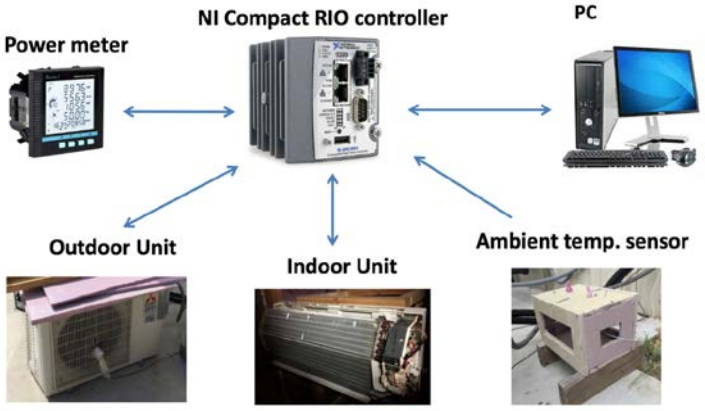

Figure 3: Experimental setup of the mini-split AC system

In our study, the manipulated inputs are condenser fan speed and evaporator fan speed. For IOC-ESC, the correlation coefficient between condenser fan speed (or evaporator fan speed) and total power consumption of the mini-split AC system are estimated, and then used as the feedback signal in the control loop. The ambient temperature is monitored by a temperature sensor located next to the outdoor unit, and the zone temperature is measured by the sensor installed inside the zone. Both the CON-ESC and IOC-ESC algorithms are implemented in LabVIEW.

4. EXPERIMENTAL RESULTS

4.1 System Calibration

Before the ESC tests, the static input-output maps are calibrated first, i.e. the map of the condenser fan speed with respect to the total power (with the evaporator fan speed set as 900 rpm) and that of the evaporator fan speed with respect to the total power (with the condenser fan speed set as 400 rpm). The zone temperature setpoint is set at 18.9 °C, and the ambient temperature varies from 29°C to 32°C. The optimal condenser fan speed is found to be around 650 rpm, and the optimal evaporator fan speed is around 900 rpm.

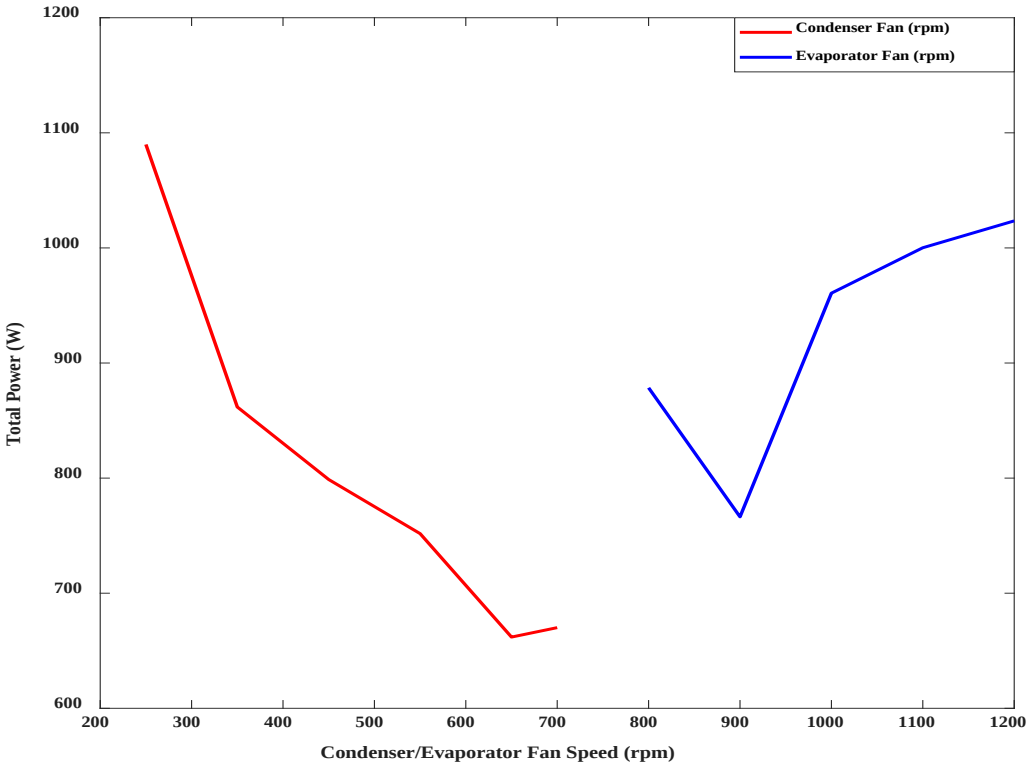

Figure 4: Static map of total power as a function of condenser and evaporator fan speed

4.2 Single-input IOC-ESC Testing

The single-input IOC-ESC is tested with the condenser fan speed as the manipulated input, while the evaporator fan speed is fixed at 900 rpm. The maximum and minimum speeds of the condenser fan speed are 750 rpm and 250 rpm, respectively. The initial condenser fan speed is set at 250 rpm. At t = 500 sec, the IOC-ESC controller with the sinusoidal dither is activated. The parameters for the IOC-ESC controller are set as follows: sampling period Δt = 1 sec, a_{norm} =0.1 a = 50 rpm) and. Experimental results of five cases are shown in Figure 5. The trajectories of zone temperature, ambient temperature, measured power consumption and condenser fan speed are plotted. The ESC input and output are normalized in the following manner: the total power is normalized by the steady-state average total power, and the condenser fan speed is normalized by the maximum condenser fan speed. The zone temperature setpoint is 19.4°C for all cases. However, the tuning parameter settings are different. For IOC-ESC#1, IOC-ESC#2 and IOC-ESC#3, TC =100 s and the dither frequency is set as 0.05/TC (0.0005 Hz), 0.1/TC (0.001 Hz) and 0.2/TC

(0.002 Hz), respectively. TF is 0.5 in these three cases. For IOC-ESC#4 and IOC-ESC#5, TC =500 s and the dither frequency is 0.25/TC (0.0025Hz) and TF is 0.05.

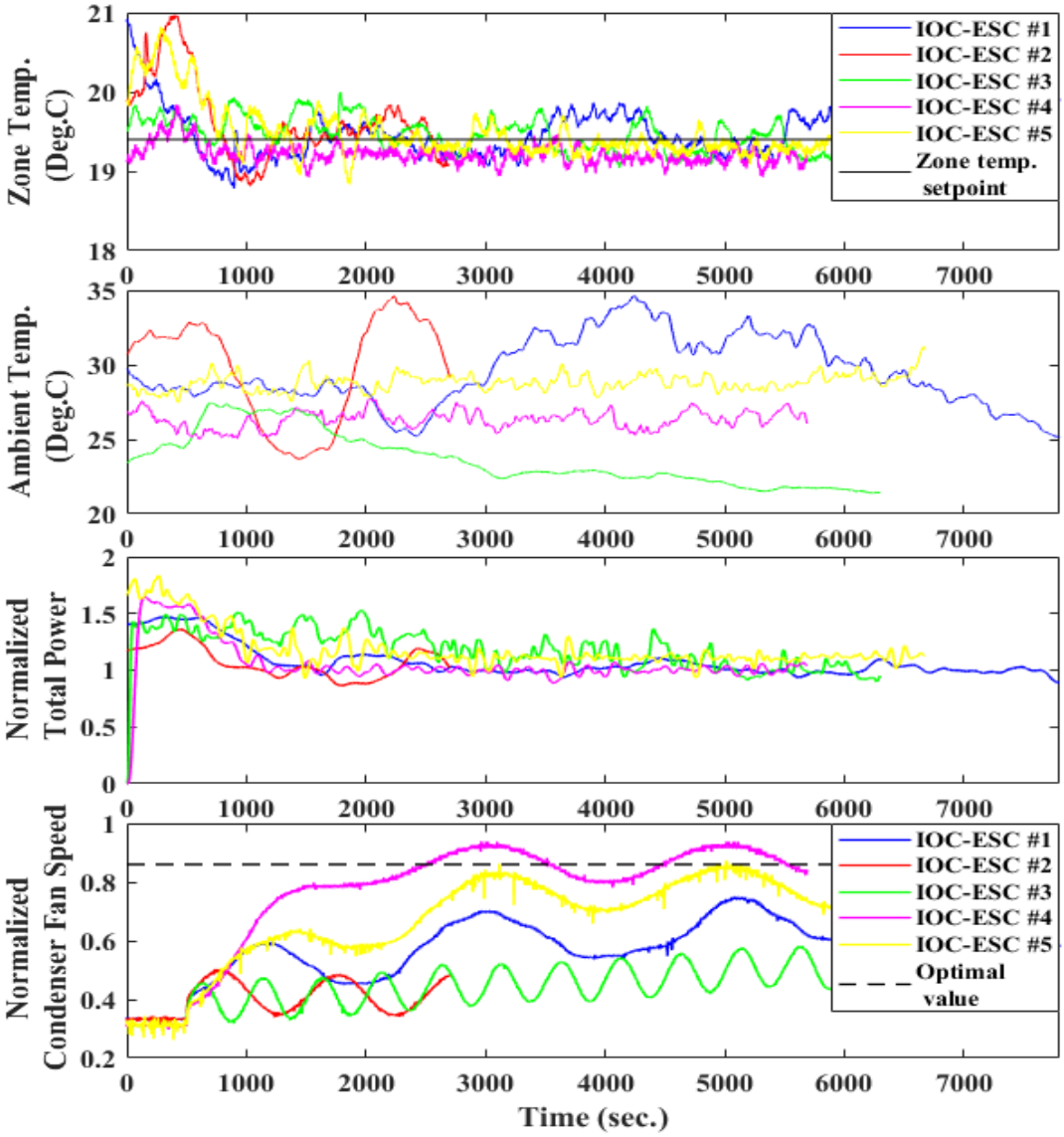

Figure 5. Testing results for single-input IOC-ESC: normalized input/output trajectories, zone and ambient temperatures.

The IOC-ESC results demonstrate the effect of two tuning parameters, i.e. the dither frequency and the tuning factor. IOC-ESC#1, IOC-ESC#4 and IOC-ESC#5 have the same dither frequency but different tuning factors, while IOC-ESC#1, IOC-ESC#2 and IOC-ESC#3 have the same tuning factor but different dither frequencies. The results reveal that the IOC-ESC performance deviates significantly from the optimum under relatively high dither frequencies, e.g. IOC-ESC#2 and IOC-ESC#3. Smaller tuning factor helps increase the convergence speed, as shown in IOC-ESC#4 and IOC-ESC#5.

Next, the CON-ESC performance is considered. The parameters are chosen based on the design guidelines provided in Xiao et al. (2014). Figure 6 shows the experimental results for two trials of CON-ESC. The initial condenser fan speed is 300 rpm for CON-ESC#1 and 250 rpm for CON-ESC#2, the dither frequency is 0.001Hz, the dither amplitude is 40 rpm and the integrator gain for the control variable is 0.002.The ESC starts at 500 sec. Based on the normalized power, the settling time of IOC-ESC ranges from 300 to 600 seconds, while the settling time of CON-

ESC ranges from 900 to 1200 seconds. Overall, the IOC-ESC converges faster than the CON-ESC based on the relatively rough estimation of setting time due to the measurement noise.

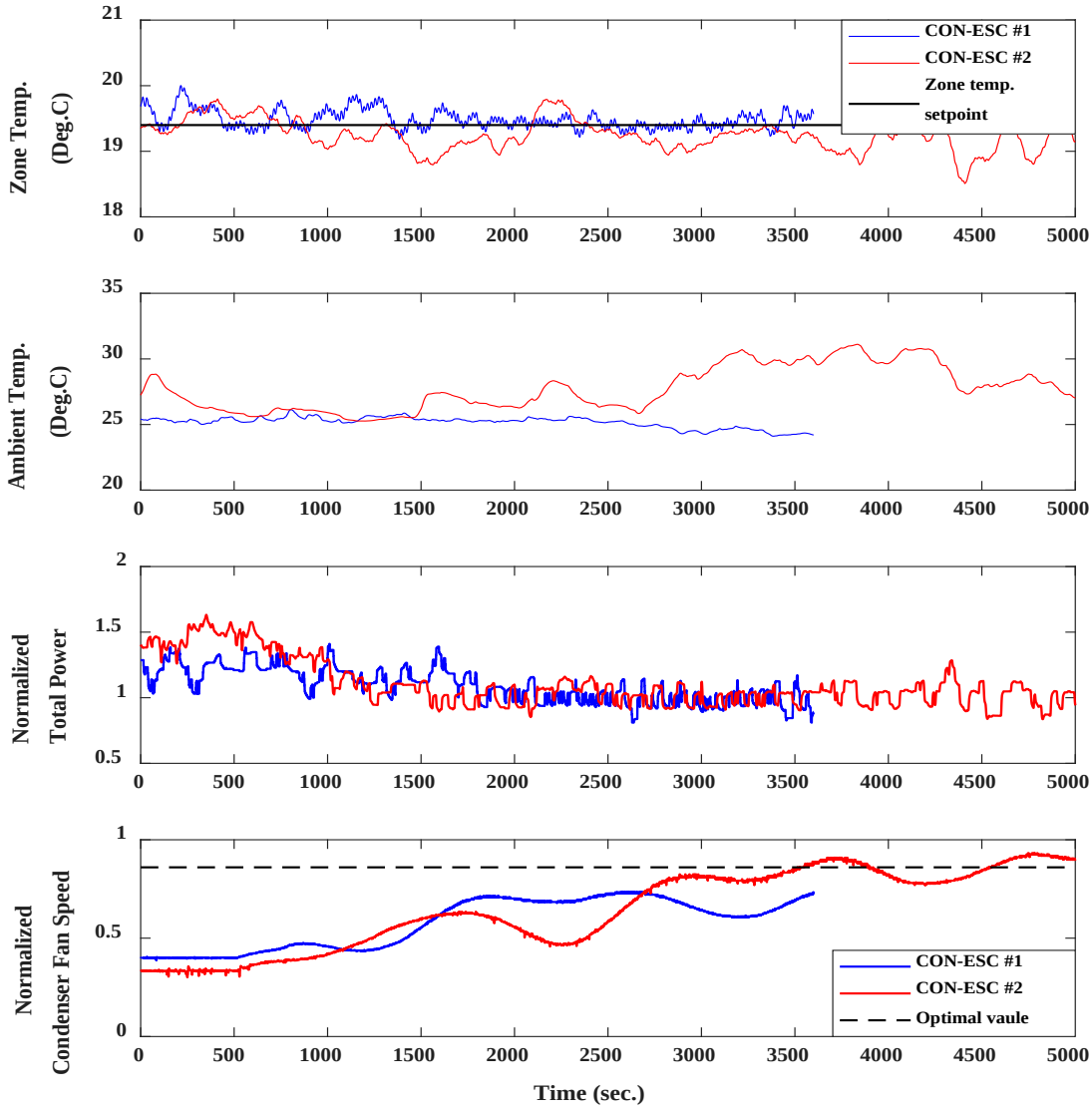

Figure 6. Testing results of single-input CON-ESC: normalized input/output trajectories, zone and ambient temperatures.

4.3 Multi-input IOC-ESC Testing

For the multi-input scenario, the manipulated inputs are condenser fan speed and evaporator fan speed. Salsbury et al. (2017) presented the IOC-ESC for the single-input case. This study extends the framework to a multivariable scenario, which is achieved by running two IOC-ESC control loops in parallel. The testing results of this two-input IOC-ESC are plotted in Figure 7. The testing results of a two-input CON-ESC using the same system are also shown in Figure 7 for comparison.

For both IOC-ESC and CON-ESC, the initial condenser fan speed and evaporator speed are set at 300 rpm and 750 rpm, respectively. The evaporator fan speed ranges from 750 rpm to 1350 rpm. The tuning parameters of two-input IOC-ESC are configured similar as the single-input cases. The sampling period is set to be 1 sec, TC is 500 s, and dither frequency is 0.25/TC (0.0025Hz) for both the evaporator and condenser fan speed channels. Other tuning parameters are different in the two channels. For the condenser fan, the amplitude a_{nor} = 0.1 (a = 50 rpm) and TF is 0.05. For the evaporator fan, the amplitude a_{nor} = 0.06 (a = 36 rpm) and the TF is 0.08. For CON-ESC, the

evaporator loop dither frequency is 0.00059 Hz, dither amplitude is 30 rpm and the integrator gain for the control variable is 0.003. While the condenser loop dither frequency is 0.00071 Hz, dither amplitude is 30 rpm and the integrator is 0.002.The zone temperature setpoint is 20°C. The CON-ESC starts at 900 sec. and converges in 1300 sec according to the normalized power. The start time of IOC-ESC is also 900 sec. while the convergence time is 900 sec. Because the ambient condition of these two tests are quite different, the convergent condenser fan speed and evaporator speed varies.

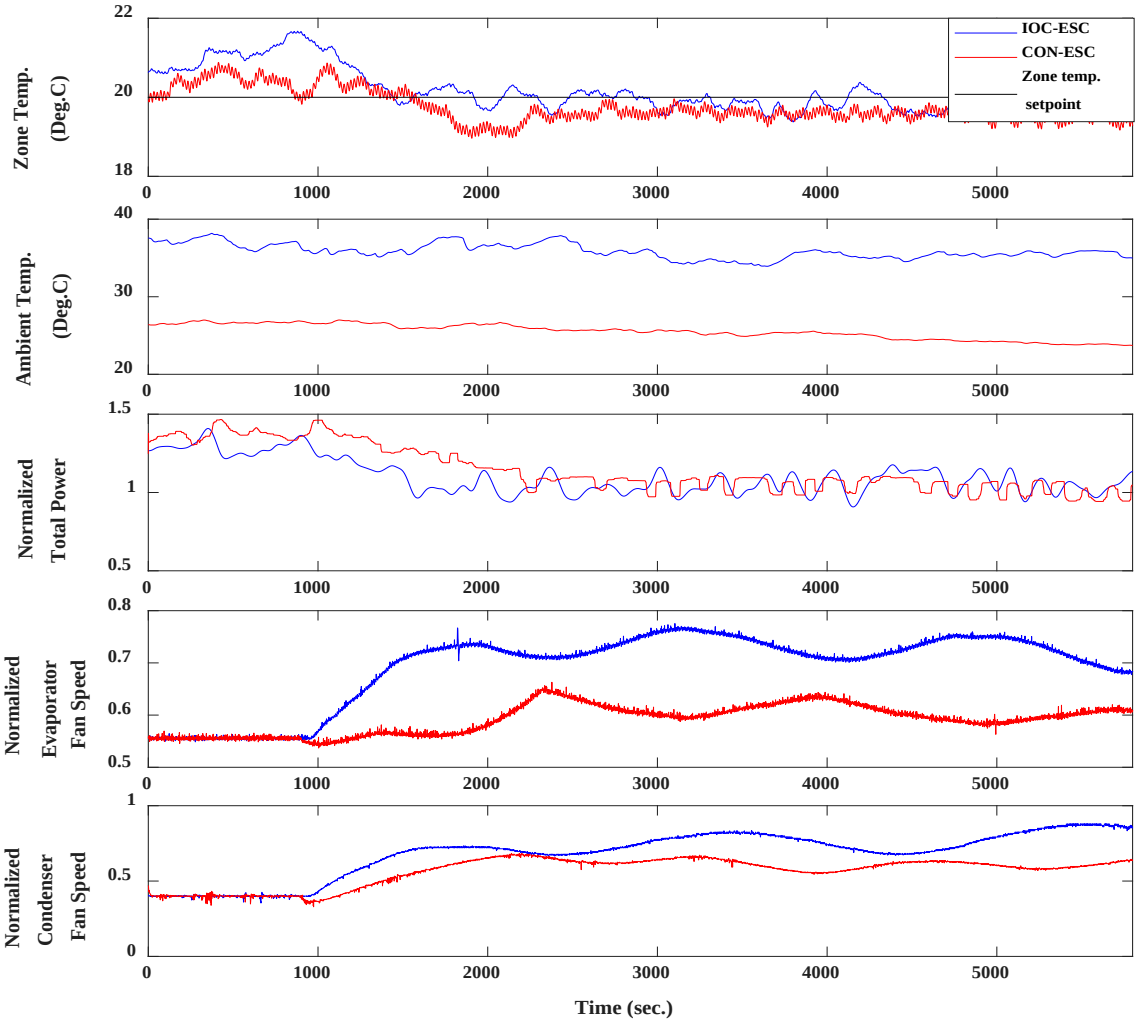

Figure 7. . Testing results of two-input IOC-ESC I/O trajectories and two-input CON-ESC

In summary, for single-input case, both of ICO-ESC and CON-ESC controllers can effectively reduce the power consumption of the mini-split system without sacrificing zone temperature regulation. However, the settling time of the CON-ESC is longer than the IOC-ESC for test cases being compared. Similarly, for two-input case, both IOC-ESC and CON-ESC can optimize the condenser fan speed and evaporator fan speed operating point practically, while the IOC-ESC converges faster.

5. CONCLUSIONS AND DISCUSSION

In this paper, an IOC-ESC is evaluated with an experimental study on a mini-split ductless AC system. Both single-input and multi-input scenarios are tested. The experimental results are compared with those of a conventional ESC. Both CON-ESC and IOC-ESC can optimize the condenser fan speed and evaporator fan speed for energy efficient operation, while the IOC-ESC converges faster and has fewer tuning parameters. The future work includes the

comparisons of more ESC algorithms and further discussion of parameter tuning required for different ESC algorithms.

ACKNOWLEDGMENTS

The authors are grateful of the financial support by Johnson Controls Inc.

REFERENCES

Tan, Y., W. H. Moase, C. Manzie, D. Nešić, and I. M. Y. Mareels. "Extremum seeking from 1922 to 2010." In *Control Conference (CCC), 2010 29th Chinese*, pp. 14-26. IEEE, 2010.

Tan, Y, D. Nešić, and I. M. Y. Mareels. "On non-local stability properties of extremum seeking control." IFAC Proceedings Volumes 38, no. 1 (2005): 550-555.

Ariyur, K.B., & Krstić, M. Multivariable extremum seeking feedback: analysis and design. In Proc. of the American control conference. 2012

Jalil, S., J, W. H. Moase, C. Manzie, Fast extremum seeking on Hammerstein plants: a model-based approach, Automatica 59 (2015)171–181.

Guay, M., and D. Dochain. "A proportional-integral extremum-seeking controller design technique." Automatica77 (2017): 61-67.

Moase, W. H., C. Manzie, M. J. Brear (2010). Newton-like extremum-seeking for the control of thermoacoustic instability. IEEE Transactions on Automatic Control, 55, 2094–2105.

Moase, W. H., C. Manzie (2011). Fast extremum-seeking on Hammerstein plants. In Proceedings of the IFAC world congress (pp. 108–113).

Gregor, G., J. P. Moeck, C. O. Paschereit, and R. King. "Advanced algorithms for gradient estimation in one-and two-parameter extremum seeking controllers." Journal of Process Control 22, no. 4 (2012): 700-709.

Hunnekens, B. G. B., M. A. M. Haring, Nathan van de Wouw, and Henk Nijmeijer. "A dither-free extremum-seeking control approach using 1st-order least-squares fits for gradient estimation." In Decision and Control (CDC), 2014 IEEE 53rd Annual Conference on, pp. 2679-2684. IEEE, 2014.

Xiao, Y, Y. Li, and J. E. Seem. "Multi-variable extremum seeking control for mini-split air-conditioning system." (2014).

Rotea, M. A. (2000). Analysis of multivariable extremum seeking algorithms. In Proceedings of the American control conference (pp. 433–437).

Ghaffari, A., M. Krstić, D. Nesic. 2012. Multivariable Newton–based Extremum Seeking. Automatica, 48: 1759-1767.

Salsbury, T. I., J. M. House, C. F. Alcala, and Y. Li. "An extremum-seeking control method driven by input–output correlation." Journal of Process Control 58 (2017): 106-116.

Finch, T., Incremental Calculation of Weighted Mean and Variance, vol. 4, University of Cambridge, 2009, pp. 11–15

Krstić, M. (2000). Performance improvement and limitations in extremum seeking control. Systems & Control Letters, 39, 313–326.

Burns, D. and C. Laughman. "Extremum seeking control for energy optimization of vapor compression systems." (2012).

Mu, B., Y. Li, and J E. Seem. "Experimental study on extremum seeking control for efficient operation of air-side economizer." (2014).

Li, P., Y. Li and J.E. Seem. 2010. Efficient Operation of Air-side Economizer Using Extremum Seeking Control. ASME Journal of Dynamic Systems, Measurement, and Control, 132(3): 031009 (10 pages).